Applications in Energy and Combustion Science 23 (2025) 100359

Contents lists available at ScienceDirect

Applications in Energy and Combustion Science

journal homepage: www.sciencedirect.com/journal/applications-in-energy-and-combustion-science

Experimental study of thermo-environmental properties of single and double-chambered bioethanol burners

Jiří Ryšavý [a,*], Estela Alexandra Domingos Vicente [b], Oleksandr Molchanov [a], Yago Alonso Cipoli [b], Kamil Krpec [a], Célia A. Alves [b], Manuel Feliciano [c,d], Imane Dargham [a], Jenn-Kun Kuo [e], Cheng-Chi Wang [e]

[a] VSB - Technical University of Ostrava, Energy and Environmental Technology Centre, Energy Research Centre, 17. listopadu 2172/15, 708 00 Ostrava-Poruba, Czech Republic
[b] Environmental and Planning Department, Centre for Environmental and Marine Studies, University of Aveiro, Campus Universitário de Santiago, 3810-193 Aveiro, Portugal
[c] Centro de Investigação de Montanha (CIMO), Instituto Politécnico de Bragança, 5300-253, Bragança, Portugal
[d] Laboratório Associado para a Sustentabilidade e Tecnologia em Regiões de Montanha (SusTEC), Instituto Politécnico de Bragança, 5300-253, Bragança, Portugal
[e] Department of Mechanical and Electro-Mechanical Engineering, National Sun Yat-sen University, 804201 Kaohsiung, Taiwan

ARTICLE INFO

Keywords:
Burner
Bioethanol
Combustion
Emissions
Indoor air quality

ABSTRACT

Bioethanol burners are becoming increasingly popular across Europe, often valued primarily for their aesthetic appeal; however, their potential role in household energy systems and their influence on the indoor environment have been largely overlooked. This study aimed to evaluate the effects of burner design, burner opening area regulation, fuel quality, and initial fuel dose on key operational and environmental performance metrics, including heat output, pollutant emission rates, and impact on indoor environment, for single- and double-chambered bioethanol burners. The results showed that single-chambered burners achieved 11–31 % higher average heat output and 8–27 % higher maximum heat output despite having a lower burner opening area. Regarding emissions, single-chambered burners exhibited lower CO emission factors (5–51 % reduction) but higher NOx emission factors (13–23 % increase) compared to double-chambered burners. Indoors, a similar trend was observed, with single-chambered burners contributing to lower CO levels but higher NOx concentrations. These findings provide new insights into how burner geometry directly affects combustion efficiency and pollutant formation mechanisms, including thermal NOx and incomplete combustion processes. This study is one of the few to combine controlled hood testing with real-room experiments, offering a comprehensive assessment of the indoor air quality implications of ethanol burner operation. The results of this study highlight the necessity for further research and development to mitigate potential health risks while maximising the efficiency of bioethanol burners as a viable household heating solution.

Introduction

The increasing global demand for sustainable and low-carbon or carbon-neutral energy sources has driven research into alternative fuels, particularly biofuels or synthetic fuels, which are considered a viable solution for reducing dependency on fossil fuels [1,2]. Among biofuels, bioethanol has gained significant attention due to its renewable nature, ease and local character of production from plenty of sources, including waste streams, easy and relatively safe treatment and potential to reduce greenhouse gas emissions [3,4]. Recent advancements in bioenergy and biofuels have highlighted the significant future potential of lignocellulosic bioethanol, with ongoing research focused on improving conversion processes and expanding the use of diverse biomass sources, particularly to reduce production costs [5,6]. Traditionally, bioethanol has been widely utilised in the transportation sector, often blended with gasoline to enhance combustion efficiency and lower pollutant emissions [7,8]. Recent studies have also provided deeper insights into the reaction kinetics of ethanol-gasoline blends, showing how ethanol chemically interacts with gasoline components to influence ignition

* Corresponding author.
E-mail addresses: jiri.rysavy@vsb.cz (J. Ryšavý), estelaavicente@ua.pt (E.A.D. Vicente), oleksandr.molchanov@vsb.cz (O. Molchanov), kamil.krpec@vsb.cz (K. Krpec), celia.alves@ua.pt (C.A. Alves), msabenca@ipb.pt (M. Feliciano), jenn.kun@mail.nsysu.edu.tw (J.-K. Kuo), wcc@ncut.edu.tw (C.-C. Wang).

https://doi.org/10.1016/j.jaecs.2025.100359
Received 14 April 2025; Received in revised form 23 June 2025; Accepted 29 July 2025
Available online 5 August 2025

Nomenclature

A_{r_C}	relative atomic mass of carbon, [-]
A_{r_H}	relative atomic mass of hydrogen, [-]
A_{r_O}	relative atomic mass of oxygen, [-]
HHV	higher heating value
k	heat of vaporisation considering the volumetric work done by the water formed from the hydrogen during combustion at 25 °C, 2.37 MJ·kg^{-1}
k_1	specific heat of water evaporation at constant pressure at 25 °C, 2.44 MJ·kg^{-1}
LHV	lower heating value, MJ·kg^{-1}; kWh·kg^{-1}
$\dot{m}_{fuel}$	fuel mass flow, kg·min^{-1}
m_{H2O}	specific mass of emitted water vapor in the flue gas, kg·kWh^{-1}
$\dot{m}_i$	pollutant mass flow, mg·min^{-1}
M_i	molar mass, kg·mol^{-1}
V_{fg}	volume flow of flue gas at STP conditions, m^3·min^{-1}
V_{m_air}	molar volume of air, dm^3·mol^{-1}
V_{m_CO2}	molar volume of CO_2, dm^3·mol^{-1}
V_{m_i}	molar volume of pollutant, dm^3·mol^{-1}
φ_i	pollutant volume fraction in the flue gas, ppm
φ_{O2_air}	volume fraction of oxygen in the air, [-]
φ_{O2_fg}	volume fraction of oxygen in the flue gas, [-]
ω_C	mass fraction of carbon in the fuel, kg·kg^{-1}
ω_H	mass fraction of hydrogen in the fuel, kg·kg^{-1}
ω_N	mass fraction of the nitrogen in the fuel, kg·kg^{-1}
ω_O	mass fraction of the oxygen in the fuel, kg·kg^{-1}
ω_w	mass fraction of the water in the fuel, kg·kg^{-1}

behaviour, particularly through OH radical competition mechanisms [9]. However, the potential of ethanol use in stationary combustion applications, particularly for household heating, and its associated implications remain relatively unexplored [10].

Bioethanol combustion in small-scale burners, implemented into bioethanol fireplaces, has gained popularity due to its aesthetic appeal, ease of operation and installation as well as for its carbon-neutral footprint [11,12]. Unlike conventional solid-fuel stoves, bioethanol burners operate without the need for a chimney (based on the producer manual), diluting flue gas into the indoor environment and making them attractive for urban dwellings with limited infrastructure [13]. Despite the advantages, concerns remain regarding the efficiency (in connection to the need for proper air exchange), heat output stability and safety (bioethanol-fuelled fireplaces have been associated with severe burn injuries, emphasising the need for improved safety measures and awareness [14,15]) and indoor air quality (IAQ) impact of these devices [16,17]. The real/incomplete combustion of bioethanol or bioethanol-based fuel can lead to emissions of carbon monoxide (CO), nitrogen oxides (NOx), total suspended particles (TSP) and organic gaseous compounds (OGC), which necessitates further research into optimising burner designs and operational parameters to minimise environmental and health risks [18,19]. The use of these devices is comparable to the use of candles, which have also been identified as a source of non-negligible pollution [20,21].

Recent studies have focused on understanding the combustion process (e.g. heat output and flue gas composition were observed) of alone-standing bioethanol burners affected by the burner opening area and fuel composition [22,23]. Research by Ryšavý et al. [24] demonstrated that modifying burner geometry can significantly impact the heat energy output, the combustion process and the amount of pollutants emitted. Furthermore, the application of oxidation catalysts, such as platinum (Pt) and palladium (Pd)-based systems, has shown promising results in reducing CO emissions while maintaining combustion stability [22]. Additional research has highlighted the impact of bioethanol appliance operation on IAQ, showing that appliance characteristics (e.g., manual or automatic ignition, nominal thermal power, closed or open fuel tank), fuel type (e.g., liquid or gel), and ventilation conditions (e.g., air changes per hour) play a key role [16,18]. These test chamber experiments have reported elevated levels of CO_2, CO, NO, NO_2, volatile organic compounds (VOCs), particles, and formaldehyde. Additionally, a study focusing on the detailed speciation of VOCs and carbonyl compounds has monitored emissions before, during, and after fireplace operation, demonstrating the significant impact of bioethanol fireplaces on IAQ and emphasising the need for widespread implementation and harmonisation of regulatory standards within the EU, such as EN 16,647 for liquid fuel fireplaces [17,25].

The present study aims to advance the scientific understanding of bioethanol burner performance by systematically investigating how burner design, opening area, fuel properties, and fuel dosing affect combustion parameters and emissions. A key novelty of this study lies in combining laboratory-based flue gas characterisation with real-room IAQ assessments—an approach rarely used in previous literature. By analysing heat output and emission behaviour under different configurations, we offer mechanistic insights into how burner structure influences pollutant formation dynamics, such as thermal NOx and products of incomplete combustion, which are critical for evaluating IAQ and health risks. The findings of this study will provide valuable insights for researchers focused on biofuels and their utilisation, as well as for manufacturers and policymakers seeking to improve the safety, efficiency, and environmental impact of bioethanol combustion appliances.

Experimental materials and equipment

Fuels

Basic information about the four different fuels is listed in Table 1. Commonly sold high-quality ethanols intended for use in bioethanol burners were chosen as the fuel for the following experiments. The manufacturers of all ethanols declared zero mass fraction of the water according to the safety datasheets available, which were connected with a given value of lower heating value (LHV) 26.9 MJ·kg^{-1} (the value for pure ethanol). The real HHVs of all fuels were measured for verification purposes by using a calorimeter (LECO AC600; USA), showing significantly lower HHV than the declared value in the case of Fuels 1, 2 and 3. In comparison, the results for Fuel 4 were almost in compliance with the reference values for pure ethanol. Each sample was measured at least five times, and the averages were taken into consideration. The obtained values of LHV were recalculated from the HHV, according to the following formula Eq. (1) given by the standard DIN 51,900–1 [24]:

$$LHV = HHV - (k \cdot 8.94 \cdot \omega_H + 0.8 \cdot (\omega_N + \omega_O) + k_1 \cdot \omega_W) \quad (1)$$

Since water was expected to be the main ballast component (taking the standard production process into consideration), its mass fraction was measured by titrator Excellence T5 (Mettler Toledo; Switzerland). Resulting values are also listed in Table 1, confirming HHV and LHV results.

The selection of fuels with varying compositions, along with their thorough physicochemical characterisation, including density, energy content, water content, and autoignition temperature, ensures a broad and representative data set. This comprehensive approach increases the relevance and transferability of the results to practical applications involving different commercial ethanol fuels used in bioethanol burners.

Additionally, the autoignition temperature of a fuel refers to the

Table 1
Properties of the tested fuels and fuel mixtures.

Fuel [–]	Density* [kg·dm^{-3}]	LHV* [MJ·kg^{-1}]	$w_{ethanol}$* [–]	$w_{propan\text{-}2\text{-}ol}$* [–]	$w_{butanone}$* [–]	w_{water}* [–]	HHV [MJ·kg^{-1}]	LHV [MJ·kg^{-1}]	w_{water} [–]	Autoignition temperature [°C]
Fuel 1	0.80 - 0.82	26.90	> 0.93	> 0.01	>0.01	–	27.710	24.917	0.058	401 ± 3
Fuel 2	n.d.	n.d.	< 0.98	< 0.06	<0.06	–	27.860	25.066	0.053	401 ± 3
Fuel 3	n.d.	n.d.	0.96	0.01	0.01	–	27.840	25.046	0.054	401 ± 3
Fuel 4	0.789	26.90	1.00	n.d.	n.d.	–	29.390	26.579	0.005	397 ± 3

Note: * Data obtained from the safety data sheet provided by the manufacturer of the fuel; w – mass share of the substance in the fuel; nd – not determined.

lowest temperature at atmospheric pressure at which the fuel will spontaneously burst into flame in the absence of an external ignition source (such as a spark or flame). These autoignition temperatures were measured in an accredited laboratory following the EN ISO/IEC 80,079–20–1 standard. The measurement utilised the Autoignition Temperature of Liquids Apparatus (AIT 551; OZM). Prior to the measurement, calibration was performed using ethanol with a purity of 99.9 %. For pure ethanol, the autoignition temperature is approximately 395 ± 3 °C. Despite the apparent similarity of Fuels 1, 2 and 3, all were used during the following experiments because differences in the amount and the type of denaturation agents can significantly influence the flue gas composition. Fuel 1 will be considered as a reference fuel for subsequent experiments.

Bioethanol fireplace and burners

For the following experiments, a commercially available bioethanol fireplace designed as a wall-mounted unit was used. For tests requiring weight loss monitoring, additional legs were constructed and mounted externally to enable freestanding operation without affecting the combustion process. The fireplace was designed to hold three separate bioethanol burners, and during all tests, three burners were always used in a consistent setup.

Two types of ethanol burners were employed during the combustion tests: single-chambered and double-chambered designs. All burners were constructed from stainless steel with a wall thickness of 2 mm and were equipped with a manually adjustable regulation flap for controlling the burner opening area.

The single-chambered burner (Fig. 1) consisted of a single internal chamber filled with ceramic wool, which absorbed the fuel uniformly after filling. Vaporisation occurred directly from the wool surface, and combustion took place above the burner as ethanol vapours were released. This design improves flame stability and enhances safety by reducing the risk of fuel spillage. Some single-chambered burners also featured a double-bottom casing to improve thermal insulation and operating safety.

In contrast, the double-chambered burner (Fig. 2) featured an internal partition that divided the fuel storage area into two sections. The first chamber, which remained empty, served as the fuel dosing area, while the second chamber, completely filled with ceramic wool, absorbed fuel gradually through a 13 mm high gap along the bottom of the partition and a series of circular orifices in its upper part. This design enabled fuel vapour to be released from both the open fuel surface in the first chamber and the saturated wool in the second chamber. As a result, flames emerged from the orifices as well as from the main opening, producing a spatially distributed combustion zone.

In both burner types, fuel vaporization was heat-assisted, primarily driven by radiant heat emitted by the flame.

The most important parameters, such as the expected heat output of each burner according to the manufacturer, burner opening area, expected heat output, etc., were listed in Table 2. Different ethanol burner designs were selected to cover a wide range of scenarios that could occur during standard household operation.

The manufacturers did not specify the conditions under which the burners' heat energy output was determined. Nevertheless, the most critical parameters influencing this value include the burner opening area (defined by the design and the position of the regulation flap), the LHV of the fuel used, and the initial fuel dose. The effects of these variables on both heat output and flue gas composition are thoroughly examined in this paper.

In terms of burner design, the observed differences in combustion efficiency between single- and double-chambered burners are primarily influenced by the geometry and internal configuration of the chambers, which affect heat transfer dynamics between the flame and burner surfaces. These design features also impact the rate and uniformity of fuel vaporisation, as well as the access to and mixing of combustion air. Together, these factors govern the overall stability and intensity of the combustion process, thereby determining the heat energy output.

The burners were equipped with a manually adjustable regulation flap, enabling control over the burner opening area. The burners were

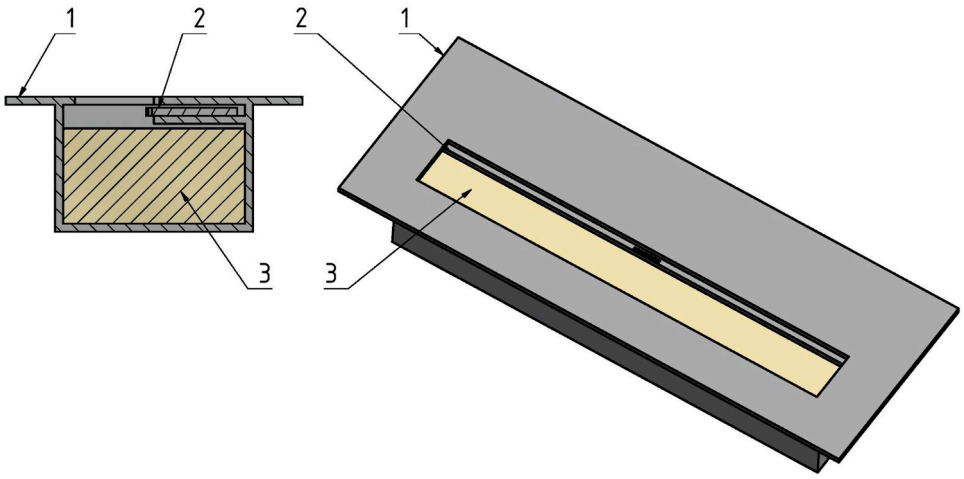

Fig. 1. Sketch of a single-chambered bioethanol burner and its section: 1—burner body, 2—regulation flap, and 3—ceramic wool [12].

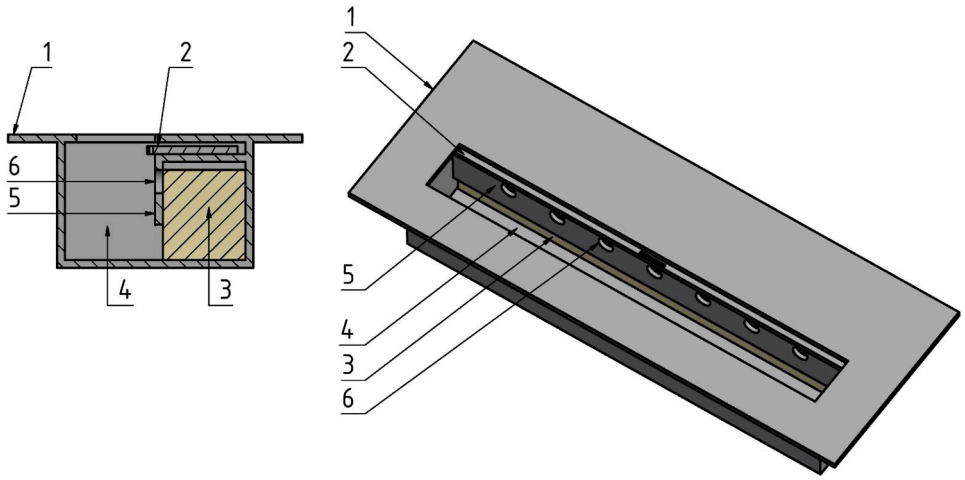

Fig. 2. Sketch of a double-chambered bioethanol burner and its section: 1—burner body, 2—regulation flap, 3—ceramic wool (second chamber), 4—empty space (first chamber), 5—wall between the chambers, and 6—circular orifice in the wall between the chambers [12].

Table 2
Main information of the bioethanol burners used in the experiments.

Bioethanol burner abbreviation	Burner designation	Burner weight	Burner opening area	Expected heat output (manufacturer's data)	Maximal initial fuel dose
[-]	[-]	[g]	[mm^2]	[kW]	[ml]
SC	Single chambered	1174	3464	1.5	200
DC	Double chambered	1528	4161	2.0	250

made of stainless steel with a material thickness of 2 mm. Ceramic wool filled approximately 2/3 of the fuel storage area. Fuel vaporisation was thermally assisted, primarily driven by radiant heat emitted from the combustion of fuel above the burner.

Testing procedure description

Hood testing

The experimental setup consists of a steel cuboid-shaped hood, within which the bioethanol fireplace was placed. The hood was purpose-built for the described experiments, with dimensions carefully selected to accommodate the entire fireplace without direct contact, maintaining approximately 1 cm of clearance on both the transverse and longitudinal sides. The hood's height (120 cm) allows proper flue gas homogenisation due to enough space between the bioethanol fireplace top and the hood ceiling. It features full rear and side walls, while the front wall was partially open to ensure unrestricted access of combustion air to the burners. The closed part of the front wall of the hood prevents flue gas leakage outside the hood and minimises unnecessary dilution by ambient air. During all combustion tests, all three slots in the bioethanol fireplace were filled, with identical setups for each burner (initial fuel dose, fuel type, regulation flap position, etc.). The experimental setup is presented in Fig. 3.

The bioethanol fireplace was placed on refractory firebricks (the legs were intentionally unused to minimise hood volume). These bricks sit atop the BL 30K1 (XS Instruments; Italy) scale. The upper part of the hood was connected to a 1.2 m long flue gas duct (160 mm in diameter) equipped with a sampling point located 30 cm above the hood ceiling. Within this sampling point, a heated probe was installed with a ceramic

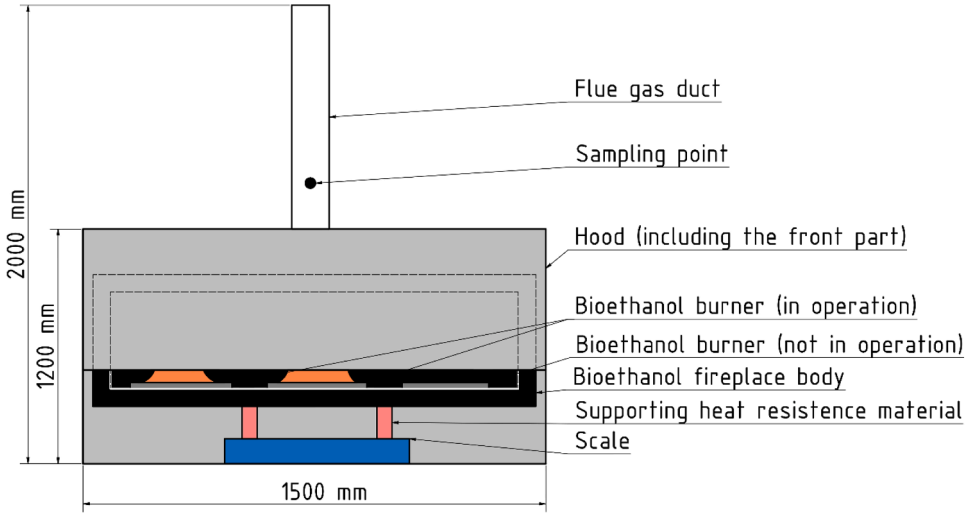

Fig. 3. Layout of the experimental setup used during hood testing.

filter, and a "T" piece allowed placement of the thermocouple right in the flue gas stream. The sample then continued through a heated hose to the external cooling device PSS 5 (M&C TechGroup; Germany). The cooled, water-free sample flows to the PG-350E (Horiba; Japan) analyser. Table 3 provides comprehensive details on the measuring instruments, their individual measurement ranges, the underlying measurement principles, and the level of accuracy. The thermocouple inserted into the heated probe was connected to the datalogger SDL200 (Extech Instruments; USA).

Room testing

The measurements were conducted in a controlled environment within a 74.34 m^3 room. The bioethanol fireplace was positioned against a wall, using the additional legs. Measurement devices were placed in the centre of the room at a height of 1.5 m above the floor to represent the breathing zone of occupants. To evaluate the effect of different burner types and fuels on IAQ, two burner configurations and two fuels (Fuel 3 and Fuel 4) were tested. The measurement protocol was designed to evaluate indoor pollutant concentrations under minimum ventilation conditions, which are typical during cold weather when doors and windows remain closed. Before the combustion tests, baseline pollutant levels were monitored to assess the impact of the bioethanol fireplace on IAQ. For each combustion experiment, the bioethanol fireplace was ignited with the burners opening fully open and the fuel reservoirs filled to near their maximum capacity (200 ml) to replicate typical usage conditions. A graduated cylinder was used to ensure the accurate addition of fuel to each burner. Additionally, one set of tests to evaluate the fuel load was conducted using Fuel 3 (250 mL) and double-chambered burners. The duration of each combustion experiment and the amount of fuel burned during each test are provided in Table 5. The end of each combustion test was defined as the moment when the flames from all three burners were extinguished. Each combustion experiment was repeated four times, on distinct days, to ensure the decay of pollutants in the room. Measurements of CO, and NOx were taken at 5-minute intervals throughout the entire experiment, covering the baseline, combustion, and post-combustion phases, using Horiba (APMA-370, APNA-370) analysers. Prior to the sampling campaign, the analysers were calibrated and validated with gas calibration bottles containing known concentrations.

Table 3
Detailed specifications of the measuring instruments, including measured components, measurement ranges, measurement principles, and accuracy levels.

Device and measured component	Range	Principle	Accuracy
Horiba PG-350E			
CO	0 – 200 ppm	NDIR	± 1 %
CO_2	0 – 10 %	NDIR	± 1 %
O_2	0 – 25 %	Paramagnetic	± 1 %
SO_2	0 – 200 ppm	NDIR	± 1 %
NO_x	0 – 50 ppm	Chemiluminescence Detection Method	± 1 %
Thermocouple, Type K, class 1			
FG temperature	- 50 to 1000 °C	Thermoelectric effect	± 1 °C

Process of the testing and data evaluation

Hood testing

Before the experiment launch, the fuel doses for all three burners were prepared separately. The scale on which the whole bioethanol fireplace lay was zeroed. After the filling of the fuel into the burners, a time gap of approximately 5 min took place for proper saturation of ethanol into the ceramic wool. Flue gas analysis and temperature measurement, as well as the weight loss record, started right at the moment of fuel ignition, which was done by a 2 kW propane-butane burner.

Following the weight loss and considering the LHV of the fuel, the heat output of the burners was determined for each minute, taking the standard EN 16,647 Fireplaces for Liquid Fuel [25] into account. Given that the flue gas (which serves as the heat energy carrier) flows directly into the ambient air within the heated room, and considering that heat losses from unburned gaseous or solid combustion products are negligible, the heat input was considered equal to the heat output. This assumption is justified by the extremely low concentrations of unburned pollutants (e.g., CO and hydrocarbons) detected in the flue gas, the complete absence of solid combustion residues, and the fact that the TSP content in the exhaust gases was found to be negligible in comparison to the total fuel mass. Therefore, nearly all the chemical energy released from the fuel during combustion was assumed to be transferred as useful thermal energy to the surrounding space.

Gas sampling started simultaneously with ignition, and all monitored flue gas parameters were continuously measured and recorded as one-minute averages. The test was terminated after the burnout of the fuel in the last burner. To obtain the actual dry flue gas flow under Standard Temperature and Pressure (STP) conditions, the theoretical flue gas flow was recalculated (based on the fuel's carbon, hydrogen, and oxygen composition) using the real volume fraction of oxygen in the flue gas as specified in Eq. (2).

$$\dot{V}_{fg} = \left(\frac{V_{m\_CO2}}{A_{r\_C}} \cdot \omega_C + \frac{\frac{V_{m\_air}}{A_{r\_C}} \cdot \omega_C + \frac{V_{m\_air}}{A_{r\_H} \cdot 4} \cdot \omega_H - \frac{V_{m\_air}}{A_{r\_O} \cdot 2} \cdot \omega_O}{\varphi_{O2\_air}} \cdot \left(\frac{\varphi_{O2\_air}}{\varphi_{O2\_air} - \varphi_{O2\_fg}} - \varphi_{O2\_air} \right) \right) \cdot \dot{m}_{fuel} \tag{2}$$

The mass flow rate of pollutants was determined by considering the measured volume fraction, molar mass, molar volume of the pollutant, and the flue gas flow under STP conditions, as specified in Eq. (3). The resulting mass concentration of NO_x in the flue gas is recalculated to NO_2.

$$\dot{m}_i = \varphi_i \cdot \frac{M_i}{V_{m\_i}} \cdot \dot{V}_{fg} \tag{3}$$

Results and discussion

Hood testing

A total of 21 combustion experiments were carried out. The details of each test setup are outlined in Table 4. These experiments were designed to examine the impact of various input parameters, including burner design, initial fuel dose, regulation flap configuration (burner opening area), and fuel quality, on both the heat energy output and the composition of flue gases. The selection of the room testing setup will be determined based on the findings from the hood testing results.

Table 4
The description of the experimental setups for the combustion tests.

No.	Burners	Fuel	Initial fuel dose for all three burners		Regulation flap setup	CO		NOx		Average heat energy output	Maximal heat energy output	Burning time
	[-]	[-]	[ml]	[g]	[%]	[mg]	[mg·kWh^{-1}]	[mg]	[mg·kWh^{-1}]	[kW]	[kW]	[hh:mm]
1	SC	Fuel 1	600	478.4	100	1037.8	312.4	292.7	88.1	3.36	4.36	1:01
2	SC	Fuel 1	450	348.3	100	768.3	316.8	210.4	86.8	3.17	4.24	0:47
3	SC	Fuel 1	300	235.1	100	663.0	404.7	145.1	88.6	3.04	4.40	0:32
4	SC	Fuel 1	150	121.1	100	397.8	471.1	61.5	72.8	2.32	3.57	0:19
5	DC	Fuel 1	750	595.1	100	1649.3	398.9	287.1	69.4	3.12	4.15	1:21
6	DC	Fuel 1	600	472.4	100	1389.9	424.7	229.7	70.2	2.98	3.90	1:07
7	DC	Fuel 1	450	356	100	1355.9	547.2	157.7	63.6	2.64	3.45	0:56
8	DC	Fuel 1	300	234.4	100	1078.0	663.3	93.0	57.2	2.16	3.20	0:43
9	DC	Fuel 1	150	112.1	100	845.6	1071.6	33.6	42.6	1.59	3.28	0:23
10	SC	Fuel 4	600	468.7	100	926.0	267.6	379.7	109.7	3.82	4.96	0:56
11	SC	Fuel 3	600	476.2	100	1019.3	305.3	303.0	90.8	3.35	4.51	1:01
12	SC	Fuel 2	600	474.6	100	1142.4	345.9	296.6	89.8	3.30	4.64	1:02
13	SC	Fuel 1	600	472.9	75	1236.3	377.7	275.2	84.1	2.54	3.28	1:20
14	SC	Fuel 1	600	473	65	d.n.b.	d.n.b.	d.n.b.	d.n.b.	d.n.b.	d.n.b.	d.n.b.
15	SC	Fuel 1	600	467.8	85	1115.5	343.5	289.4	89.1	2.91	3.61	1:09
16	DC	Fuel 1	750	595.4	75	d.n.b.	d.n.b.	d.n.b.	d.n.b.	d.n.b.	d.n.b.	d.n.b.
17	DC	Fuel 1	750	595.8	65	d.n.b.	d.n.b.	d.n.b.	d.n.b.	d.n.b.	d.n.b.	d.n.b.
18	DC	Fuel 1	750	595.6	85	1735.3	421.0	266.1	64.6	2.73	3.74	1:33
19	DC	Fuel 4	750	597.9	100	1801.2	405.7	375.1	84.5	3.48	4.78	1:20
20	DC	Fuel 3	750	591.1	100	1800.1	437.4	318.7	77.4	3.20	4.51	1:19
21	DC	Fuel 2	750	592.6	100	1775.4	428.3	312.4	75.4	3.22	4.30	1:20

Note: d.n.b. – does not burn.

The volume fraction of oxygen in the flue gas, which was significantly influenced by its dilution by excess air, ranged between 21 % (beginning and the end of the combustion process) and 20 % (peak of the combustion phase). In general, a lower volume fraction of oxygen in the flue gas was achieved when using the maximum fuel dose, Fuel 4, with a higher LHV and a fully opened burner opening area. On the contrary, decreasing the initial fuel dose amount, using fuels with lower LHV, or partially closing the burner opening area led to higher O_2 concentrations. The volume fraction of oxygen in the flue gas, which was significantly influenced by its dilution by excessing air ranged between 21 % (beginning and the end of the combustion process) and 20 % (peak of the combustion phase). In general, lower volume fraction of the oxygen in the flue gas were reached in the case of usage maximal fuel dose, Fuel 4 with higher LHV and fully opened burner opening area. On the contrary decreasing of the initial fuel dose amount, usage of the fuels with lower LHV or partial close of burner opening area led towards higher reached oxygen volume fraction in the flue gas. The results presented confirm that the hood design did not restrict the access of combustion air in any way.

Influence of the burner design on the combustion process parameters

For this purpose, experiments no 1, 5 and 6 can be compared experiment 1 and 5 represent the state of maximal initial fuel dose in both burners, while experiments 1 and 6 share the same initial fuel dose in both burners. The heat energy output curves as well as the curves representing increment of the NOx emitted are shown in Fig. 4.

As evident from the results, the single-chambered burners achieved 7 % and 11 % higher average heat output, respectively, compared to the double-chambered burners when filled to maximum capacity (250 ml) or the same capacity as the single-chambered burners (200 ml). In terms of maximum heat energy output, the increases were approximately 5 % and 10 %, respectively. This difference is also associated with shorter burning times in the case of single-chambered burners (1h01), about 20 and 6 min shorter, respectively. These results align with the findings of Ryšavý et al. [12], who used a significantly reduced initial fuel dose (60 % and 48 %) for the same bioethanol burner.

The heat energy output curve shows a rapid increase during the first minute, which is characteristic for bioethanol fireplaces, although the peak in the first minute was below the level of an average heat energy output for the entire test. This was followed by a gradual rise in heat energy output over approximately 40 min, likely due to the heating up of the bioethanol burners, which simultaneously accelerates fuel vaporisation. Both the single-chambered burner with the maximum reference fuel dose and the double-chambered burner with 200 ml of fuel

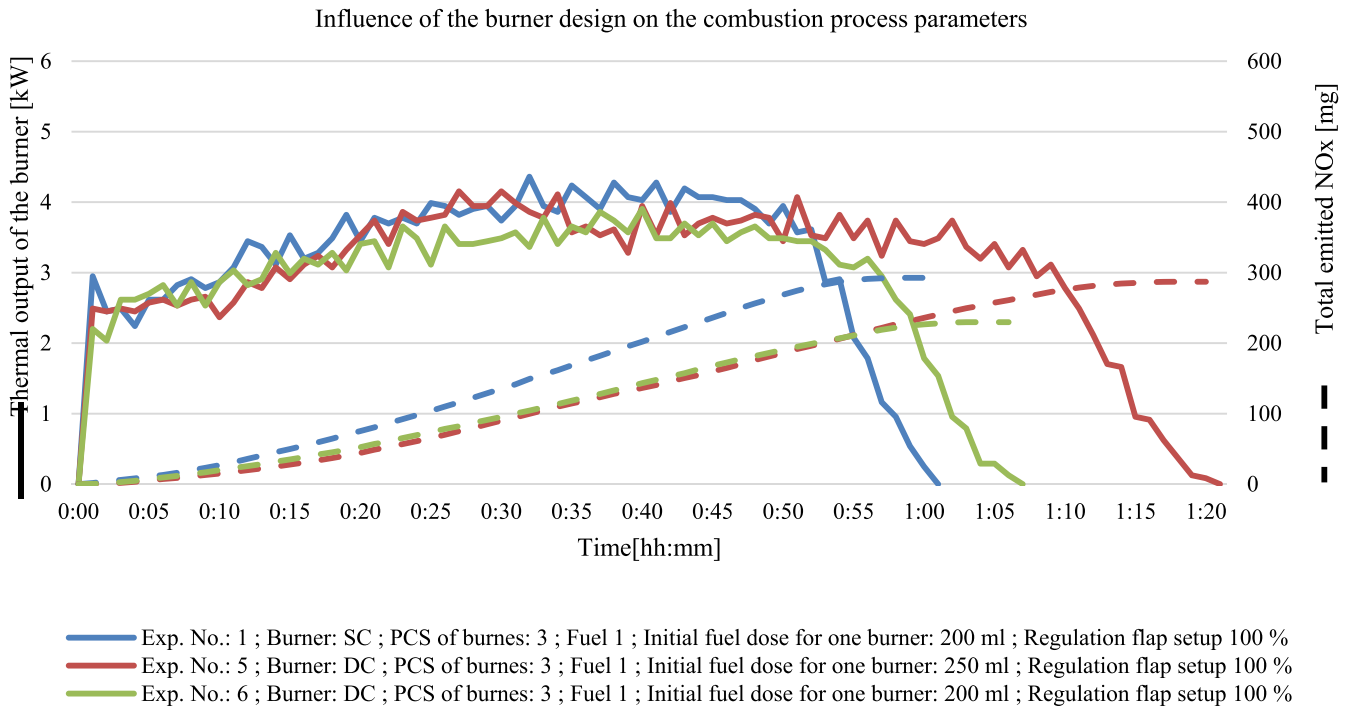

Fig. 4. Influence of burner design on the combustion process parameters – heat energy output, NOx emissions (single chambered burners).

maintained a high heat energy output level without any significant drop until the burnout phase after reaching maximum heat-up. However, in the case of the double-chambered burner with 250 ml of fuel, a decrease in heat output was observed around the midpoint of the experiment, likely due to the depletion of fuel in the first chamber, which was not absorbed by the ceramic wool in the second chamber. The single- and double-chambered burners exhibit a slightly different heat output pattern compared to the vortex-flame bioethanol burner (without the limitation on the burner opening area), which quickly reaches the maximum heat energy output (in the first minute after ignition) followed by a continuous decrease throughout the duration of the test [24].

The emission factor for CO, as presented in Table 4, was lowest when using single -chambered burners, while the double-chambered burners exhibited higher values, by approximately 27 % and 35 %, respectively. The higher CO emissions observed in double-chambered burners may be attributed to less effective air-fuel mixing and localised oxygen-deficient zones during combustion, which hinder the complete oxidation of CO to CO_2. In contrast, the more open configuration of single-chambered burners likely promotes more uniform combustion, thereby reducing CO formation [26]. In contrast, the NOx emission factors showed an inverse trend: the single-chamber burners recorded the highest values, while the double-chamber burners demonstrated lower values around 21 % and 20 %, respectively. The NOx emission rate of the single-chambered burner was significantly more noticeable than that of the double-chambered burner, which showed similar increment rates for both 200 and 250 ml initial fuel doses throughout the experiment without significant difference (only the main combustion phase was longer in the case of a higher fuel dose). NOx emission was formed continuously during the combustion process except the burnout phase, with lower emission rates after the ignition and gradually increasing formation rate with increasing heat energy output. During nitrogen-free fuel combustion, only thermal and, at specific conditions of localised fuel-rich conditions, prompt NOx formation can occur. The overall high air excess ratio and elevated temperatures suggest that NOx formation is primarily driven by the thermal mechanism, which dominates under oxygen-rich and high-temperature conditions—particularly in the case of single-chambered burners. The relatively higher flame temperatures and shorter flame quenching distances in these burners could promote increased thermal NOx generation through the Zeldovich mechanism [27]. Kiang et al. [19] provide a detailed explanation of the possible NO_x formation mechanisms. From a fluid dynamics perspective, the presence of a dividing wall in double-chambered burners can interrupt the laminar flow of vaporized ethanol, potentially leading to lower combustion temperatures in localised regions. This effect may explain the slightly reduced NOx formation despite comparable heat outputs in some test cases [28]. The impact of bioethanol on combustion properties and emissions in internal combustion engines has been well-documented, supporting the findings on NOx and CO emissions in this study [29].

Since this test focused on the basic burner setup and reference fuel, a comparison with, for example, a vortex-flame burner is relevant. In terms of NOx emission factors, the vortex-flame burner exhibited values approximately ten times higher than those of the single and double-chambered burners. Under the reference settings, the heat energy output per 1 mm^2 of opening area for the vortex-flame burner ranged between 0.45 and 0.71 $W{\cdot}mm^{-2}$, compared to 0.32 and 0.25 $W{\cdot}mm^{-2}$ for both the single and double-chambered burners. Such a high heat energy output for an area in a vortex-flame burner causes high NOx emissions and almost no CO emissions, except during the ignition and burnout phases, which are very short in the vortex-flame burner. This is primarily attributed to the high excess of combustion air and the high temperatures achieved in the combustion area [24].

The placement of the burners in the bioethanol fireplace operating at the reference setup appears to be less suitable in terms of overall NOx emissions, with an increase of approximately 50 %. This finding aligns with the previous study by Ryšavý et al. [22], where two single-chambered burners, positioned side by side as free-standing units, were evaluated. However, from the perspective of CO emissions, it is a more favourable arrangement, showing a reduction to nearly one-quarter of the presented value.

In the broader context of bioethanol combustion devices, the NOx emission factors reported in this study are lower than those found in previous work by Sileghem et al. [30], where bioethanol used in a spark ignition combustion engine operating with a low air excess ratio and

high combustion temperatures, produced NOx emissions of 9 to 19 g·kWh^{-1}, depending on the ethanol's water content. In comparison, NOx emission factors for wood log stoves range from 360 to 475 mg·kWh^{-1}, while pellet combustion in stoves or boilers results in NOx emission factors between 215 and 260 mg·kWh^{-1}, as reported by Ozgen et al. [31]. However, it must be added that the mentioned sources release flue gas into the outdoor environment, whereas bioethanol fireplaces emit their combustion productsdirectly into the indoor environment.

From a fluid dynamics perspective, the double-chambered burner introduces an internal barrier that alters vapour flow, potentially leading to stratified combustion zones. This partitioning can cause uneven temperature distribution and localised oxygen deficiency, which may explain the higher CO emissions and reduced thermal NOx formation. However, at the same time, these conditions may also enable prompt NOx formation. In contrast, the single-chambered design allows for more homogeneous vapour release and better mixing with ambient air, promoting complete combustion but increasing NOx due to higher localised temperatures.

Influence of the fuel quality on the combustion process parameters

For this purpose, experiments no 1, 10, 11, and 12 can be compared for the single-chambered burners, while experiments no 5, 19, 20, and 21 are relevant for the double-chambered burners. The mentioned experiments represent the combustion process with the same initial fuel dose (by volume), allowing for the evaluation of fuel quality on the flue gas composition and heat energy output. The heat energy output curves, as well as the curves representing the increment of the NOx emitted, are shown in Fig. 5 for single-chambered burners and in Fig. 6 for double-chambered burners.

As shown in Fig. 5, the results for fuels 1, 2, and 3 show minimal differences in burning time (1 and 2 min) and NOx emissions (4 and 11 mg) across both burner designs. However, in the double-chamber burner, fuel 1 emitted slightly less NOx compared to fuels 2 and 3. This difference is associated with a lower maximum heat output—0.15 kW and 0.36 kW less than that of fuels 2 and 3, respectively. A similar trend was observed in the single-chamber burner, where fuel 1 produced a maximum heat output that was 0.28 kW and 0.15 kW lower than fuels 2 and 3, respectively. Nevertheless, the slower decline in heat output towards the end of the combustion process resulted in almost identical NOx emissions across all three fuels at the end of the combustion process.

Fuel 4, which had the highest HHV among all the fuels, achieved the highest maximum heat outputs (4.96 kW for the single-chamber burner and 4.78 kW for the double-chamber burner) and the highest average heat outputs (3.82 kW and 3.43 kW, respectively). This resulted from faster and more intense self-heating of the burner during operation, leading to quicker fuel evaporation and, thus, higher heat energy output. In the single-chamber burner, this also resulted in a shorter burning time, with the burnout phase being 4 min shorter. However, this effect was not observed in the double-chamber burner, where the dividing wall between the chambers significantly decreased the influence of the fuel's calorific value on the evaporation rate from the rear chamber. This is also evident from the smaller differences between average and maximum heat energy output for fuels 1, 2 and 3 and fuel 4 in the case of the double-chambered burner than in the case of the single-chambered burner, where the differences were more significant.

This behaviour can be further explained by considering the influence of burner geometry on fuel vapour flow and air mixing. The geometry of the single-chamber burner enables more open and continuous vapour release, which likely promotes improved mixing between vaporised ethanol and combustion air [32,33]. In contrast, the double-chamber design introduces a partition that disrupts the uniform flow of fuel vapours, potentially causing regions of incomplete mixing and localised oxygen deficiency. These conditions are conducive to incomplete combustion, as supported by the higher CO emissions observed in the double-chamber burner. This pattern is consistent with fluid dynamics principles, where internal barriers reduce turbulence and delay air-fuel mixing in low-pressure diffusion combustion environments.

Differences in fuel quality, particularly the water content,alter evaporation kinetics, which in turn influence combustion temperature and the formation of pollutants. Fuels with higher heating values accelerate vaporisation and combustion rates, intensifying thermal gradients that favour NOx formation, a trend consistent with established combustion theory [4]. The higher combustion temperature of the fuel with higher HHV led to the formation of a larger amount of NOx. Emission factors during combustion of fuel 4 were higher, ranging from about 21 to 25 % in the case of the single-chambered burner and from about 9 to 21 % in the case of the double-chambered burner. These

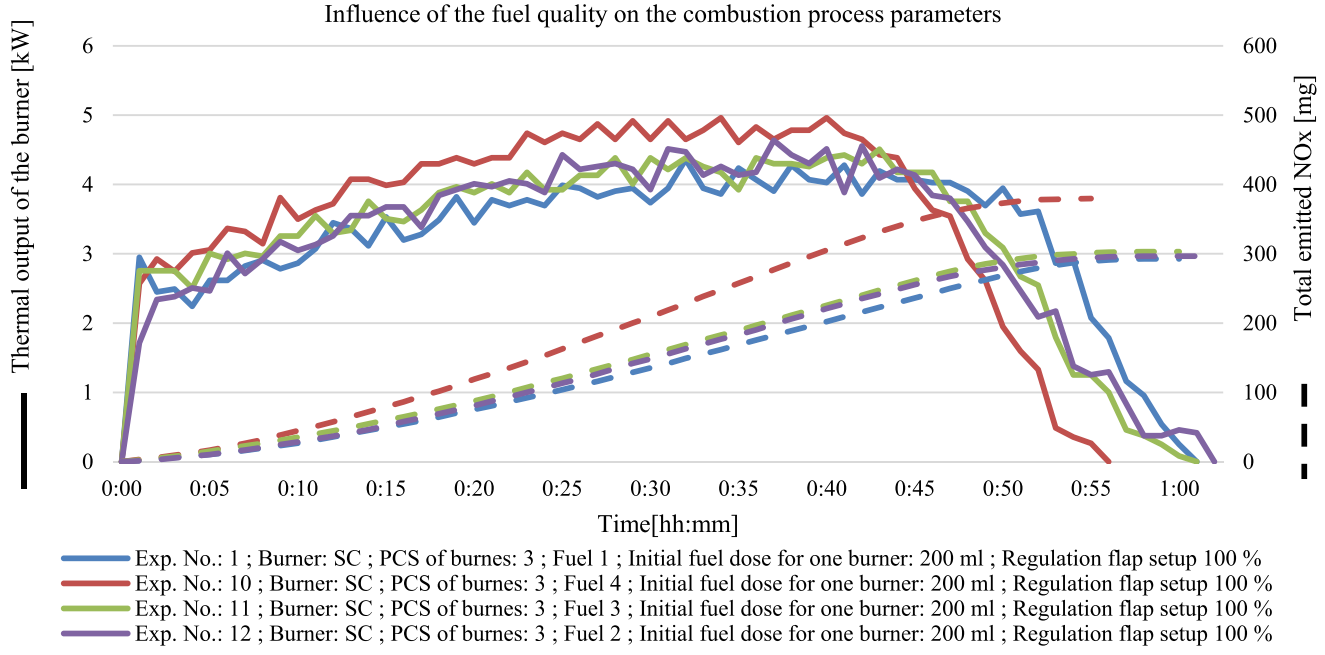

Fig. 5. Influence of the fuel quality on the combustion process parameters – heat energy output, NOx emissions (single chambered burners).

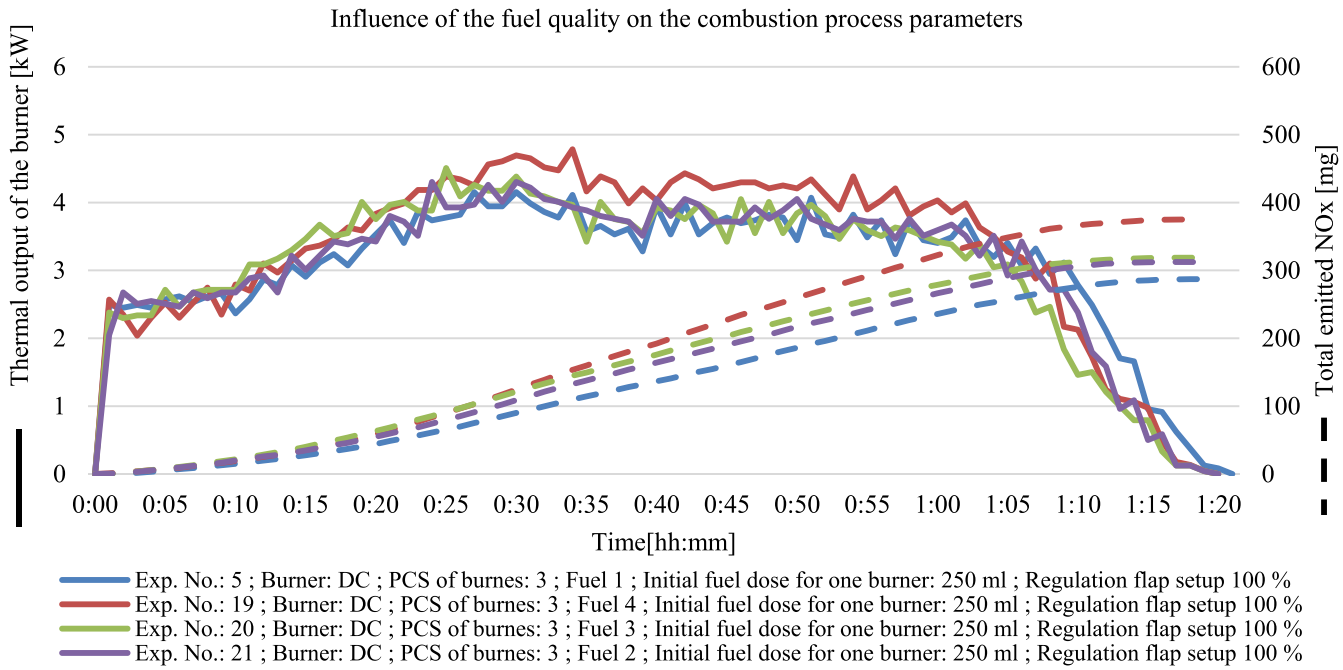

Fig. 6. Influence of the fuel quality on the combustion process parameters – heat energy output, NOx emissions (double chambered burners).

findings are consistent with the results described in our previous study, where it was observed that lower heat energy output caused by using less calorific fuel (ethanol/methanol and ethanol/water blends) is correlated with reduced NOx emissions, both in terms of total emitted pollutant and emission factor [22].

Regarding CO emissions, the single-chamber burner tests with fuels 1 and 3 produced consistent results, with overall emissions around 1025 ± 10 mg, as is shown in Table 4. Most CO was emitted during the ignition and especially the burnout phases. In contrast, the test with fuel 2 emitted a higher CO mass of 1142 mg, largely due to the prolonged burnout phase (visible in Fig. 5), where a 4-minute delay before complete burnout was observed. Conversely, fuel 4, with the highest HHV, resulted in the lowest CO emissions. The more intense combustion and higher flame temperature led to a more complete combustion process, which simultaneously led to higher amounts of emitted NOx. This effect was not observed in the double-chamber burner, where the lowest CO emissions were recorded with fuel 1.

From an emissions factor perspective, the single-chamber burner consistently showed lower CO emission factors for all fuels, while the double-chamber burner produced lower NOx emission factors in the case of comparison of the same fuels.

Influence of the regulation flap setup on the combustion process parameters

To evaluate the influence of the regulation flap setup on combustion parameters, experiments no 1, 13, 14, and 15 for the single-chamber burner, and experiments no 5, 16, 17, and 18 for the double-chamber burner, were compared. All experiments used the same initial fuel dose (by volume), enabling a direct comparison of the flap's impact on

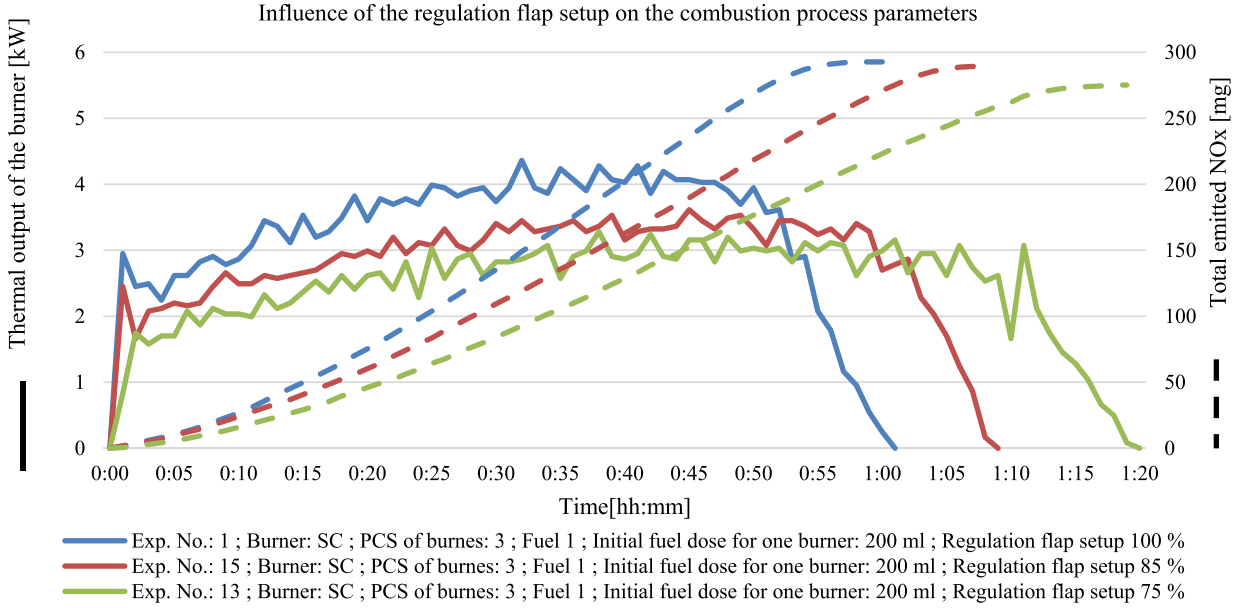

Fig. 7. Influence of the regulation flap setup on the combustion process parameters – heat energy output, NOx emissions (single chambered burners).

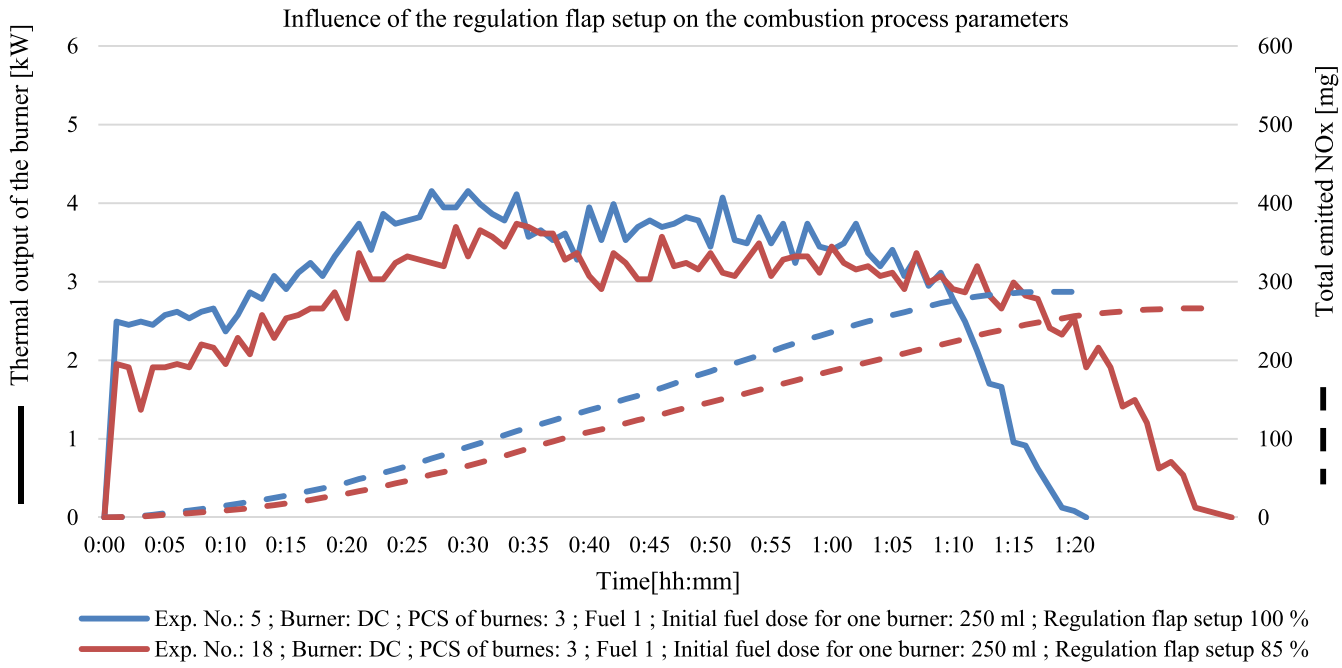

Fig. 8. Influence of the regulation flap setup on the combustion process parameters – heat energy output, NOx emissions (single chambered burners).

flue gas composition and heat energy output. The heat output curves, and NOx emission increments are displayed in Fig. 7 for the single-chamber burner and in Fig. 8 for the double-chamber burner.

In accordance with the testing plan, the regulation flap was gradually closed in steps (85 %, 75 %, and 65 %) up to 65 % of the burner's maximum opening area. Initial results indicated that combustion could be sustained up to 75 % of the maximum opening area for the single-chamber burner, while for the double-chamber burner, combustion was maintained only up to 85 %. Any further reduction in the opening area led to the interruption of combustion a few seconds after ignition or prevented ignition entirely, even after at least five attempts. The inability to sustain combustion below certain flap openings suggests a critical dependence on air-fuel ratio for flame stability. According to combustion theory, excessively low burner openings lead to rich mixtures and inadequate entrainment of oxygen, resulting in flame quenching [34].

In comparison, the vortex-flame bioethanol burner allowed regulation of the burner opening area down to 32 %, as demonstrated by Ryšavý et al. [24], whereas both the single- and double-chamber burners exhibited significantly more limited ranges of adjustment. Reducing the opening area to 85 % resulted in a decrease in maximum heat output by approximately 17 % for the single-chamber burner and 10 % for the double-chamber burner, while average heat output dropped by 13 % and 12 %, respectively. A further reduction to 75 % caused a 25 % drop in both maximum and average heat output for the single-chamber burner.

The average heat output of the single-chamber burner appeared to decrease linearly as the regulation flap was continuously closed within its operational range. Due to this limited regulation range, it is difficult to directly compare the results with those of the vortex-flame bioethanol fireplace, which exhibited a polynomial relationship between average heat output and burner opening area but over a significantly wider range of adjustment [24]. Szegö et al. [35] also noted a non-linear relationship between heat output and air-fuel ratios in their experiments, underscoring the complexity of combustion dynamics.

Reducing the burner opening area extended the operation time by approximately 13 % and 31 % for the single chamber burner when the closing flap setup was reduced to 85 % and 75 %, respectively. For the double chamber burner, a reduction to 85 % extended the operation time by about 14 %.

These results can be compared with previously published findings on a vortex flame bioethanol burner, where reducing the burner opening area to 67.7 % also extended the burning time by approximately 14 %. The impact of limiting the burner opening area on operation time is more pronounced for single- and double-chamber burners. However, vortex flame burners allow for significantly greater reductions in the burner opening area—up to 32.45 %—compared to the limitations of single- and double-chamber burners, which are restricted to reductions of 75 % and 85 %, respectively [24].

Regarding NOx emissions, it is evident that the lower heat output resulting from the partial closure of the regulation flap led to a reduction in the emission rate of this pollutant. However, due to the longer burning duration, the total amount of NOx emitted during tests remained almost identical for the single-chamber burner. A slight decrease in emissions, around 6 %, was observed only at the 75 % burner opening setting, which was linked to a reduced tendency for thermal nitrogen oxides formation. In contrast, for the double-chamber burner, reducing the regulation flap to 85 % resulted in a total NOx emission reduction of about 7 %.

Conditions of regulated average heat energy output were favourable for CO formation causing increasement of emission factors by 10 and 21 % in the case of single chambered burner and increasement of 6 % in the case of double chambered burner.

Influence of the initial fuel dose on the combustion process parameters

To evaluate the influence of the initial fuel dose on combustion parameters, experiments no 1, 2, 3 and 4 for the single-chamber burner, and experiments no 5, 6, 7, 8 and 9 for the double-chamber burner, were compared.

The heat output curves, and NOx emission increments are displayed in Fig. 9 for the single-chambered burner and in Fig. 10 for the double-chambered burner.

The impact of the initial fuel dose on the combustion process was evaluated for both single-chambered and double-chambered burners under identical conditions, with the regulation flap fully open (100 % opening area). Experiments 1 and 5, which represent the highest fuel doses for the single-chambered and double-chambered burners, respectively, serve as reference ones for the subsequent comparison of

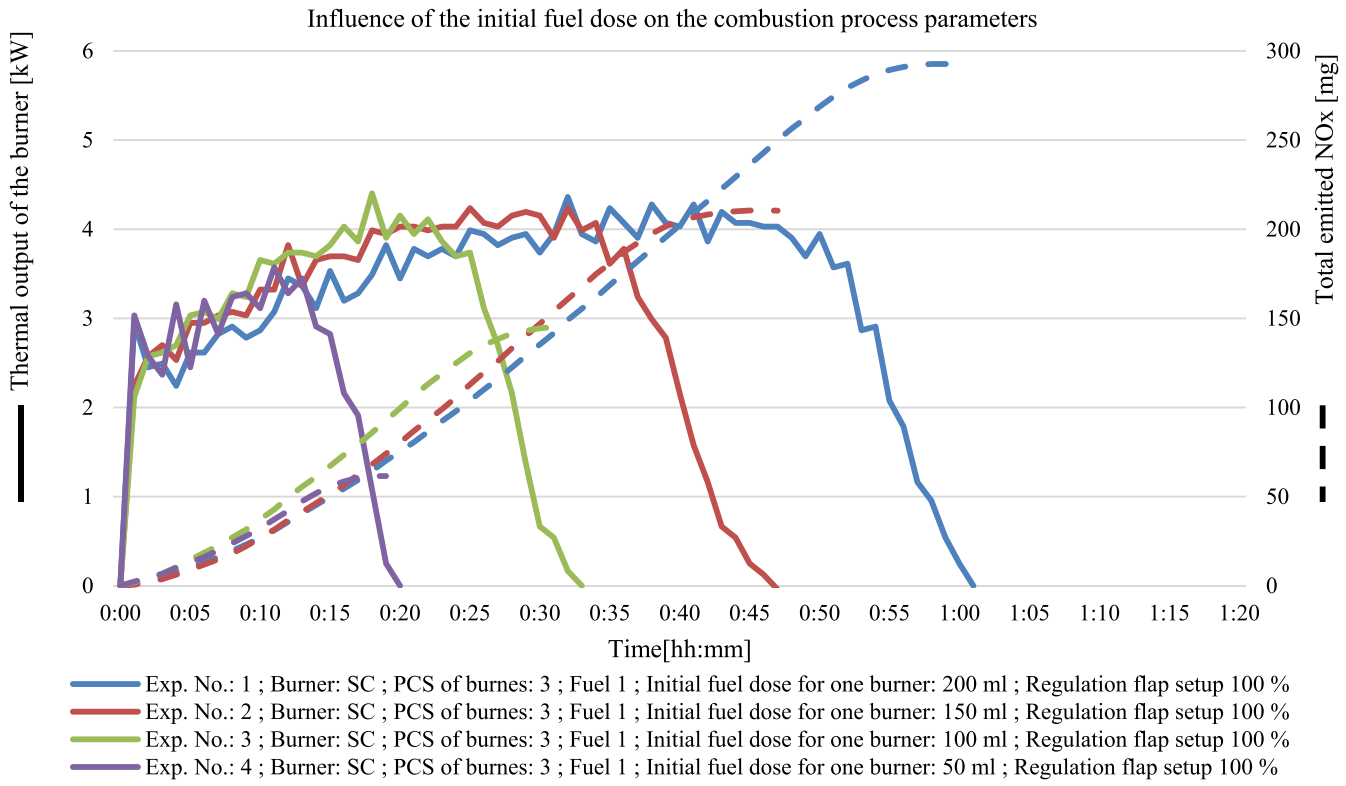

Fig. 9. Influence of the regulation flap setup on the combustion process parameters – heat energy output, NOx emissions (single chambered burners).

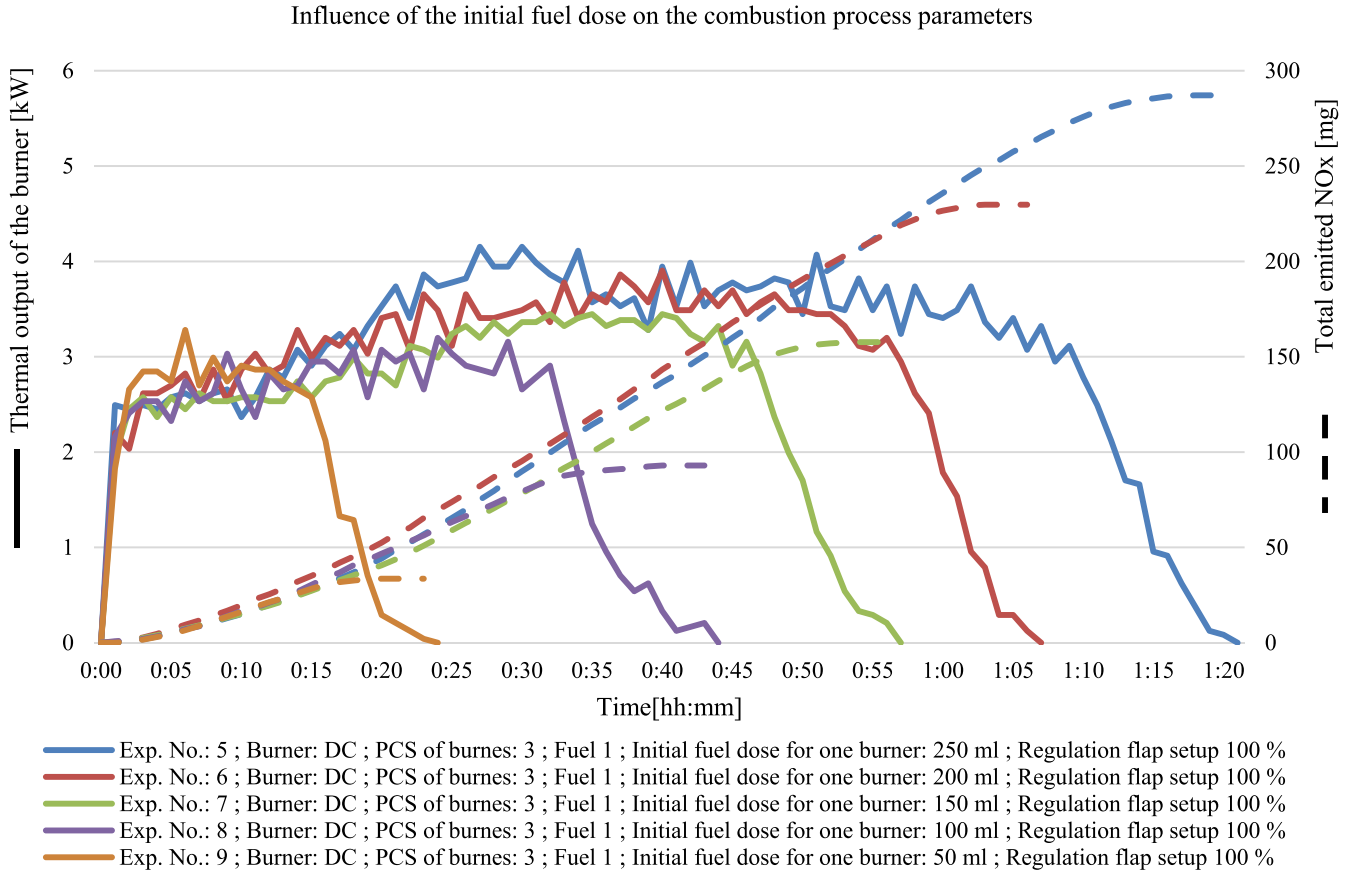

Fig. 10. Influence of the regulation flap setup on the combustion process parameters – heat energy output, NOx emissions (double chambered burners).

heat output and flue gas composition across varying initial fuel doses. For the single-chambered burner, reducing the initial fuel dose from 200 ml in experiment 1 to 50 ml in experiment 4 significantly influenced combustion behaviour. The burning time decreased from time 1:01 in experiment 1 to 0:19 in experiment 4, representing a 69 % reduction. The average heat energy output dropped from 3.36 kW in experiment 1 to 2.32 kW in experiment 4, reflecting a 31 % decline. Similarly, the maximal heat output decreased by 18 %, from 4.36 kW to 3.57 kW. This was mainly due to the burner operation time. At lower fuel doses, the heat output in the first phase of the combustion process was similar to the reference one, but early fuel burnout prevented the entire growth portion of the heat output curve from being reached.

In terms of pollutants, CO emission factors rose by 51 % compared to experiment 1, reaching 471.1 mg·kWh^{-1} in experiment 4. On the other hand, NOx emissions exhibited a significant decline, dropping by 17 % from 88.1 mg·kWh^{-1} in experiment 1 to 72.8 mg·kWh^{-1} in experiment 4. This reduction is probably due to the lower flame temperatures reached, which were associated with reduced fuel availability. This was related to the slower fuel vaporisation (advanced combustion phases are typically accompanied by faster vaporization and, therefore, burning of the fuel) and, therefore, a richer fuel/air mixture. This observation is supported by the study of Cui et al. [36], which found that CO emissions increase and NOx emissions decrease when the fuel-rich flame is adjusted.

The double-chambered burner showed similar trends as the fuel dose decreased from 250 ml in experiment 5 to 50 ml in experiment 9. The burning time decreased from 1:21 in experiment 5 to 0:23 in experiment 9, a reduction of 72 %, which aligns with the pattern observed for the single-chambered burners. The average heat output declined from 3.12 kW in experiment 5 to 1.59 kW in experiment 9, marking a 49 % decrease. The maximal heat output showed a smaller reduction of 21 %, from 4.15 kW to 3.28 kW. CO emission factors increased sharply with decreasing fuel doses, rising from 398.9 mg·kWh^{-1} in experiment 5 to 1071.6 mg·kWh^{-1} in experiment 9, an increase of 169 %. Conversely, NOx emissions significantly declined, dropping by 38 % from 69.4 mg·kWh^{-1} in experiment 5 to 42.6 mg·kWh^{-1} in experiment 9.

Comparing the two burners, the single-chambered burner consistently delivered slightly higher heat outputs at equivalent fuel doses. The single-chambered burners exhibited shorter burning times across all experiments. In terms of emissions, the double-chambered burners performed better at high fuel doses, producing 28 % lower CO emissions in experiment 5 compared to the single-chambered burner in experiment 1 (398.9 mg·kWh^{-1} versus 312.4 mg·kWh^{-1}). However, at lower fuel doses, the double-chambered burner generated significantly higher CO emissions. For example, in experiment 9, CO emissions were 127 % higher than those of the single-chambered burners in experiment 4.

Overall, the single-chambered burners were more effective at maintaining higher heat outputs, while the double-chambered burners exhibited better emission control at higher fuel doses. These findings underline the critical influence of burner design and fuel dosing on combustion efficiency and environmental impact. The data reveal a trade-off between maximal/average heat energy output and pollutant formation, a phenomenon well-documented in combustion literature. While higher fuel doses and opening areas enhance heat output, they also create thermal conditions conducive to NOx formation, underscoring the importance of balancing thermal and environmental performance in burner design.

Room testing

A total of 20 combustion experiments were conducted, with the specific details of each setup presented in Table 5. The experiments were designed to evaluate the effects of burner design, initial fuel load, and fuel quality on IAQ. The combustion duration generally ranged from 59 min to about 1 hour and 20 min, depending on the burner and fuel load. The double-chambered burner tended to sustain slightly longer combustion durations, probably due to the slower burn rate associated with this burner design.

The average indoor CO concentrations during the combustion experiments ranged between 2.48 ± 1.42 ppm (Fuel 4, SC burners) and 5.19 ± 2.24 ppm (Fuel 3, DC burners). On average, these levels were 16 to 34 times higher than the background concentrations (0.15 ± 0.02 ppm), respectively. Regarding NO_X indoor levels, the highest average concentration was recorded for Fuel 4 in the single-chamber burner setup (0.63 ± 0.41 ppm), while the lowest was observed for Fuel 3 in the double-chamber burner (0.53 ± 0.27 ppm). Background NO_x levels ranged from 0.004 to 0.006 ppm.

The maximum average concentrations of CO and NOx measured during the experiments, approximately 5 ppm of CO and 0.7 ppm of NO_X, carry significant implications for IAQ and human health. These pollutants are known to have adverse effects, even at low concentrations, particularly in enclosed spaces such as those where bioethanol fireplaces are used. According to health guidelines set my international organisms such as the World Health Organisation (WHO), the U.S. Environmental Protection Agency (EPA) and the California Ambient Air Quality Standards, exposure to 5 ppm of CO for 1 hour is within acceptable limits for IAQ. However, prolonged exposure from repeated

Table 5
Indoor CO and NOx concentrations during the combustion period for experiments with different setups.

Test	Fuel [-]	Burners [-]	Initial fuel dose for all three burners [ml]	Regulation flap (%) [%]	CO [ppm]	NOx [ppm]	Burning time [hh:mm]
#1	Fuel 3	DC	250	100	4.98 ± 2.46	0.67 ± 0.38	01:20
#2	Fuel 3	DC	250	100	5.05 ± 2.22	0.64 ± 0.33	01:19
#3	Fuel 3	DC	250	100	5.04 ± 2.29	0.66 ± 0.34	01:18
#4	Fuel 3	DC	250	100	5.31 ± 2.19	0.66 ± 0.31	01:19
#1	Fuel 3	SC	200	100	2.76 ± 1.48	0.59 ± 0.35	01:04
#2	Fuel 3	SC	200	100	2.60 ± 1.39	0.58 ± 0.36	01:05
#3	Fuel 3	SC	200	100	2.64 ± 1.47	0.58 ± 0.37	01:05
#4	Fuel 3	SC	200	100	2.61 ± 1.41	0.58 ± 0.35	01:05
#1	Fuel 3	DC	200	100	5.01 ± 2.17	0.52 ± 0.27	01:12
#2	Fuel 3	DC	200	100	5.11 ± 2.29	0.52 ± 0.27	01:12
#3	Fuel 3	DC	200	100	5.23 ± 2.33	0.53 ± 0.28	01:15
#4	Fuel 3	DC	200	100	5.42 ± 2.40	0.54 ± 0.28	01:13
#1	Fuel 4	DC	200	100	4.22 ± 2.03	0.61 ± 0.39	01:03
#2	Fuel 4	DC	200	100	4.39 ± 1.97	0.60 ± 0.36	01:04
#3	Fuel 4	DC	200	100	4.53 ± 2.09	0.62 ± 0.38	01:03
#4	Fuel 4	DC	200	100	–	–	01:03
#1	Fuel 4	SC	200	100	1.07 ± 0.77	0.20 ± 0.19	01:04
#2	Fuel 4	SC	200	100	2.43 ± 1.27	0.64 ± 0.37	01:03
#3	Fuel 4	SC	200	100	2.74 ± 1.47	0.70 ± 0.42	00:59
#4	Fuel 4	SC	200	100	2.79 ± 1.49	0.72 ± 0.43	01:00

use or poor ventilation can cause symptoms like headaches, dizziness, and fatigue [37].

NOx, particularly nitrogen dioxide (NO_2), is a respiratory irritant that can exacerbate conditions such as asthma and bronchitis and reduce lung function over time. The measured NO_x concentration of 0.7 ppm exceeds both the WHO's recommended hourly exposure limit of 0.1 ppm and the California Ambient Air Quality Standard of 0.18 ppm, indicating potential health risks with prolonged or repeated exposure. Short-term exposure to NOx can cause airway inflammation and increase susceptibility to respiratory infections. Long-term exposure, even at lower levels, can contribute to chronic respiratory diseases and a decline in overall lung health [38].

These results are consistent with the findings of Schripp et al. [18], who investigated emissions from ethanol fireplaces in a 48 m^3 test chamber. Their study demonstrated that NO_X levels exceeded guideline values in all tested setups (four ethanol fireplaces with 8 different fuels), whereas CO concentrations remained within the established limits. Guillarme et al. [14] investigated bioethanol combustion using various fireplace and fuel combinations, finding that CO concentrations exceeded the INRS ED 984 limits for occupational exposure to chemical agents in France in three out of the four setups tested.

The temporal analysis of the data reveals that both CO and NO_X concentrations followed a consistent daily pattern across the various combustion days (Fig. 11 and Fig. 12). Pollutant levels steadily increased, reaching peak concentrations towards the end of the combustion period, followed by a gradual decline over approximately 6 to 7 h until returning to baseline levels, similar to those recorded at the beginning of the experiments.

Both the burner type and bioethanol fuel choice significantly influence CO and NO_x levels during fireplace operation. Results consistently showed that NO_x peak and average concentrations were higher when using the single-chamber burner compared to the double-chamber burner, regardless of the bioethanol fuel used. In contrast, CO peak and average levels were higher with the double-chamber burner. The choice of bioethanol fuel had a notable impact on indoor NOx peak levels, while CO peak concentrations remained similar across fuels. Combustion of fuel 4 consistently produced higher NOx levels than fuel 3 (Table 5), regardless of the burner type used. This indicates that the composition or purity of the fuel can significantly alter the emission profile. This observationis supported by Ryšavý et al. [22], who reported that NOx emissions were highest during the combustion ofpure ethanol but decreased significantly when ethanol was mixed with water. Their study showed that NOx emissions decreased by 43 % with an 80/20 ethanol-water mixture and by 25 % with a 90/10 mixture. This reduction in NOx emissions was attributed to the reduction in flame temperatures resulting from the addition of water to ethanol, thereby suppressing thermal NOx formation. Since NOx formation in nitrogen-free fuel combustion occurs primarily through thermal and prompt mechanisms, lower combustion temperatures directly reduce the potential for thermal NOx production. This is consistent with the findings of the present study. The measured NOx concentration peaks are approximately half of those reported by Nozza et al. [16] This discrepancy is attributed todifferences in room dimensions, ventilation rate and heat energy output of the burners.

In addition to burner design and fuel type, the amount of fuel loaded into the burner was found to impact the emission of CO and NO_X. Higher fuel loads (Fuel 3, 250 ml) produced slightly increased indoor CO and NOx concentrations during combustion. This suggests that fuel quantity can influence the combustion dynamics, potentially leading to higher combustion temperatures and increased formation of thermal NOx.

The combination of elevated CO and NOx concentrations in indoor environments can pose cumulative health risks, especially for vulnerable populations such as children, the elderly, and individuals with preexisting respiratory or cardiovascular conditions. Effective mitigation strategies include ensuring adequate ventilation during bioethanol fireplace use, optimising burner designs to minimise emissions, and incorporating catalytic converters or air filtration systems to reduce pollutant levels. Proper fireplace design can reduce partial heat loss caused by ventilation immediately following burnout, as shown by Ryšavý et al. [10].

Conclusions

The study emphasises the significance of burner construction in

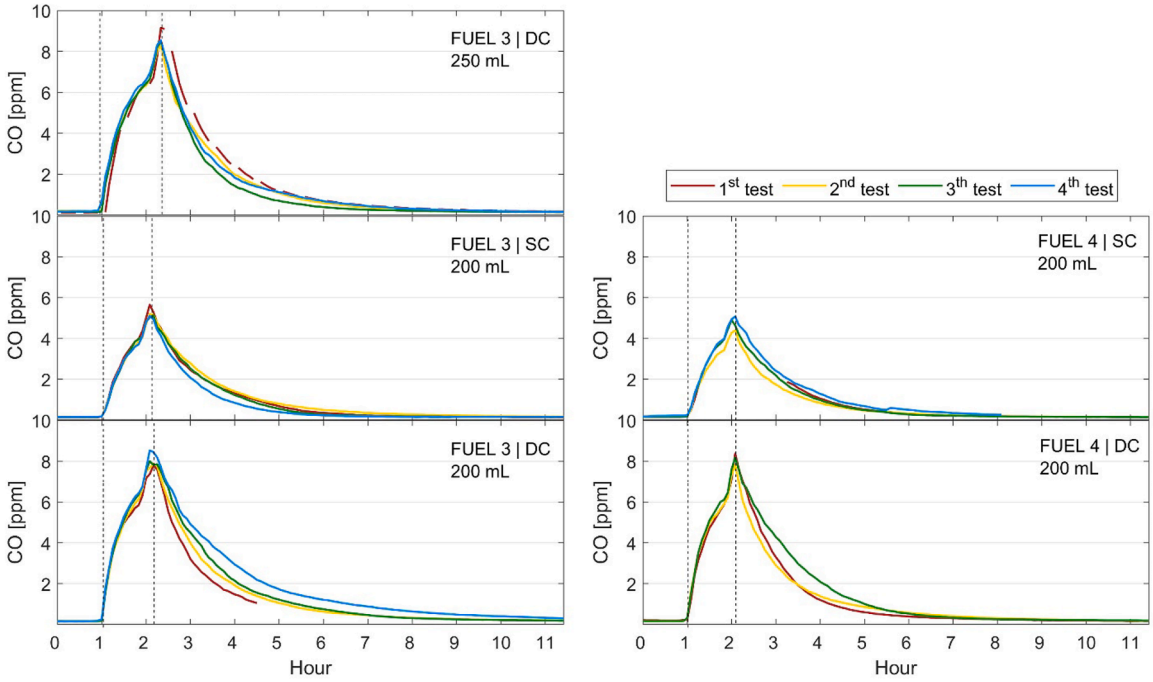

Fig. 11. Indoor CO concentration profiles (ppm) measured before, during, and after the operation of the bioethanol fireplace under various conditions across different sampling days. The combustion period is indicated by a dashed line.

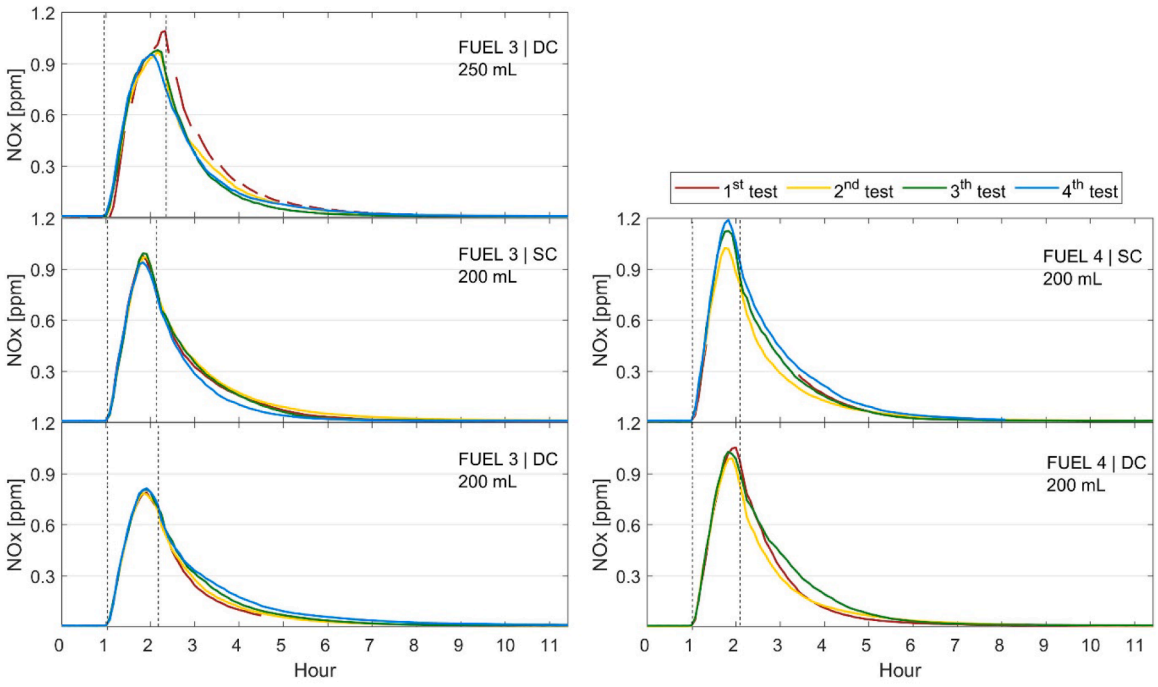

Fig. 12. Indoor NOx concentration profiles (ppm) measured before, during, and after the operation of the bioethanol fireplace under various conditions across different sampling days. The combustion period is indicated by a dashed line.

bioethanol fireplaces and its impact on combustion parameters and pollutant emissions. The comparative analysis between single-chambered and double-chambered ethanol burners provides valuable insights into optimising combustion performance and minimising emissions.

The single-chambered burner, serving as a baseline, demonstrated consistent combustion performance under standard conditions. However, the introduction of the double-chambered burner design, with its enhanced vapoured fuel flow dynamics through a separated combustion chamber structure, resulted in notable differences in the combustion course. Specifically, the double-chambered burner reduced NOx emissions by 13 – 23 % compared to the single-chambered burner across various operational scenarios and the exact initial fuel dosage. From the CO emission factors point of view, chambered burner represents significantly worse results, about 5 – 51 %. Moreover, the single-chambered burner proved to have a higher regulation range of up to 75 % of the burner opening area, as well as a higher heat energy output point of view. Differences in commercially available fuel quality were found to be a significant influencing factor for both CO and NOx emissions, as well as the heat energy output.

Real-life experiments performed in a controlled room environment supported the hood testing results, including the influences observed with higher calorific fuels as well as the amount of initial fuel dose, while highlighting the importance of air ventilation during bioethanol burner operation.

These findings highlight the direct influence of burner geometry and operational parameters on combustion efficiency and pollutant formation pathways. By identifying trade-offs between CO and NOx emissions and linking them to burner design, this study contributes new knowledge in combustion science applicable to low-pressure, diffusion-limited systems. The dual approach—combining laboratory flue gas analysis with real indoor measurements—sets a precedent for the holistic evaluation of household biofuel appliances. Future research should explore additional burner configurations, the integration of secondary measures for flue gas purification, and the use of alternative fuels to enhance combustion efficiency further and reduce environmental impact. The findings obtained from the room experiments underscore the importance of balancing the aesthetic and functional benefits of bioethanol fireplaces with their potential impact on indoor air quality and, therefore, human health.

These findings align with the principles of combustion optimisation, where burner geometry, airflow dynamics, and fuel properties must be tuned collectively to achieve the desired performance. The observed trends provide empirical validation for theoretical models that describe the formation of pollutants in low-pressure, diffusion-controlled combustion systems.

By advancing the understanding of bioethanol combustion dynamics, this study contributes to the development of cleaner, more efficient heating solutions, aligning with global efforts to mitigate indoor air pollution and promote sustainable energy practices.

CRediT authorship contribution statement

Jiří Ryšavý: Writing – original draft, Validation, Methodology, Funding acquisition, Formal analysis, Data curation, Conceptualization. **Estela Alexandra Domingos Vicente:** Writing – original draft, Validation, Methodology, Investigation, Formal analysis, Data curation, Conceptualization. **Oleksandr Molchanov:** Writing – review & editing, Methodology. **Yago Alonso Cipoli:** Writing – review & editing, Investigation, Formal analysis, Data curation. **Kamil Krpec:** Writing – review & editing, Methodology. **Célia A. Alves:** Writing – review & editing, Methodology. **Manuel Feliciano:** Writing – review & editing, Investigation, Formal analysis. **Imane Dargham:** Writing – original draft, Methodology, Investigation. **Jenn-Kun Kuo:** Writing – review & editing, Supervision. **Cheng-Chi Wang:** Writing – review & editing, Supervision.

Declaration of competing interest

The authors declare that they have no known competing financial interests or personal relationships that could have appeared to influence the work reported in this paper.

Acknowledgements

This work was financed by the project LIFE-IP SK Air Quality Improvement (LIFE18 IPE/SK/000010), supported by funding from the LIFE Programme of the European Union. Part of the work was financed by national funds in Portugal through FCT – Fundação para a Ciência e a Tecnologia I.P., under the project/grant UID/50006 + LA/P/0094/2020. In addition, FCT is acknowledged for the research contract under Scientific Employment Stimulus to Estela D. Vicente (DOI: 10.54499/2022.00399.CEECIND/CP1720/CT0012) Yago A. Cipoli (SFRH/BD/04992/2021) also acknowledges FCT for the PhD scholarship.

Data availability

Data will be made available on request.

References

[1] Dorian JP, Franssen HT, Simbeck DR. Global challenges in energy. Energy Policy 2006;34(15):1984–91.
[2] Čespiva J, Wnukowski M, Skřínský J, Perestrelo R, Jadlovec M, Výtisk J, et al. Production efficiency and safety assessment of the solid waste-derived liquid hydrocarbons. Env Res 2024;244:117915. C7.
[3] Bergthorson JM, Thomson MJ. A review of the combustion and emissions properties of advanced transportation biofuels and their impact on existing and future engines. Renew Sustain Energy Rev 2015;42:1393–417.
[4] Kun-Balog A, Sztankó K, Józsa V. Pollutant emission of gaseous and liquid aqueous bioethanol combustion in swirl burners. Energy Convers Manag 2017;149:896–903.
[5] Guo M, Song W, Buhain J. Bioenergy and biofuels: history, status, and perspective. Renew Sustain Energy Rev 2015;42:712–25.
[6] Zabed H, Sahu J, Suely A, Boyce A, Faruq G. Bioethanol production from renewable sources: current perspectives and technological progress. Renew Sustain Energy Rev 2017;71:475–501.
[7] Stančin H, Mikulčić H, Wang X, Duić N. A review on alternative fuels in future energy system. Renew Sustain Energy Rev 2020;128:109927.
[8] Costa RC, Sodré JR. Hydrous ethanol vs. gasoline-ethanol blend: engine performance and emissions. Fuel 2010;89(2):287–93.
[9] Zhang J, Morsch P, Minwegen H, vom Lehn F, Wu X, Alexander Heufer K, et al. Insights into the underlying reaction kinetics of gasoline–ethanol interactions and their effects on the auto-ignition characteristics of gasoline/ethanol blends. Appl Energy Combust Sci 2025;22:100333. C7.
[10] Ryšavý J, Horák J, Krpec K, Hopan F, Kuboňová L, Molchanov O. Heat energy accumulation construction for bioethanol burner. Energy Rep 2023;9:107–14.
[11] Neubrech F, Kiefer J, Schmidt VJ, Bigdeli AK, Hernekamp JF, Kremer T, et al. Domestic bioethanol-fireplaces–a new source of severe burn accidents. Burns 2016;42(1):209–14.
[12] Ryšavý J, Horák J, Kuboňová L, Hopan F, Krpec K, Kubesa P, et al. Real operating parameters of bioethanol burners in terms of heat output. ACS Omega 2020;5(44):28587–96.
[13] Šproho S. Bio Flame; 2020. Available from: https://www.biokrb-levne.cz/ [Accessed 4 March 2020].
[14] Guillaume E, Loferme-Pedespan N, Duclerget-Baudequin A, Raguideau A, Fulton R, Lieval L. Ethanol fireplaces: safety matters. Saf Sci 2013;57:243–53.
[15] van Zoonen E, van Eck I, van Baar M, Vries A, van Schie C, van der Vlies C. Aetiology of bioethanol related burn accidents: a qualitative study. Burns 2024;50(3):733–41.
[16] Nozza E, Capelli L, Eusebio L, Derudi M, Nano G, Del Rosso R, et al. The role of bioethanol flueless fireplaces on indoor air quality: focus on odour emissions. Build Env 2016;98:98–106.
[17] Höllbacher E, Ters T, Rieder-Gradinger C, Srebotnik E. Emissions of indoor air pollutants from six user scenarios in a model room. Atmos Env 2017;150:389–94.
[18] Schripp T, Salthammer T, Wientzek S, Wensing M. Chamber studies on nonvented decorative fireplaces using liquid or gelled ethanol fuel. Env Sci Technol 2014;48(6):3583–90.
[19] Kiang Y-H. Chapter 8 - Combustion process characterization for fuels, biomass, wastes, biosludge, and biocarbons. fuel property estimation and combustion process characterization. Academic Press; 2018. p. 265–312.
[20] Fappiano L, Caracci E, Iannone A, Murru A, Avino P, Campagna M, et al. Emission rates of particle-bound heavy metals and polycyclic aromatic hydrocarbons in PM fractions from indoor combustion sources. Build Env 2024;265.
[21] Hu H, Ye J, Liu C, Yan L, Yang F, Qian H. Emission and oxidative potential of PM2.5 generated by nine indoor sources. Build Env 2023:230.
[22] Ryšavý J, Horák J, Krpec K, Hopan F, Kuboňová L, Molchanov O. Influence of fuel mixture and catalyst on the ethanol burner flue gas composition. Energy Rep 2022;8:871–9.
[23] Millán-Merino A, Fernández-Tarrazo E, Sánchez-Sanz M, Williams FA. A multipurpose reduced mechanism for ethanol combustion. Combust Flame 2018;193:112–22.
[24] Ryšavý J, Jaroch M, Horák J, Krpec K, Molchanov O, Bury M, et al. Bioethanol burner operating parameters optimization: effects of burner opening area modulation on heat output and flue gas composition. Energy Convers Manag: X 2024;23:100616.
[25] CEN. Fireplaces for liquid fuels. *Decorative appliances producing a flame using alcohol based or gelatinous fuel - Use in private households.* en 16647: 2015. Comite Europeen de Normalisation; 2015. p. 36.
[26] Mörtberg M, Blasiak W, Gupta A. Combustion of normal and low calorific fuels in high temperature and oxygen deficient environment. Combust Sci Technol 2006;178(7):1345–72.
[27] Rao A, Liu Y, Ma F. Study of NOx emission for hydrogen enriched compressed natural along with exhaust gas recirculation in spark ignition engine by Zeldovich' mechanism, support vector machine and regression correlation. FUEL 2022:318.
[28] Józsa V. Mixture temperature-controlled combustion: a revolutionary concept for ultra-low NOX emission. FUEL 2021:291.
[29] Grzelak PL, Chłopek Z, Szczepański K. Properties of substitute motor fuels produced from ethanol in biorefineries. Combust Engines 2024;198(3):41–7.
[30] Sileghem L, Casier B, Coppens A, Vancoillie J, Verhelst S. Influence of water content in ethanol-water blends on the performance and emissions of an si engine. In: FISITA 2014 World Automotive Congress - Proceedings; 2014.
[31] Ozgen S, Caserini S, Galante S, Giugliano M, Angelino E, Marongiu A, et al. Emission factors from small scale appliances burning wood and pellets. Atmos Env 2014;94:144–53.
[32] MaKJaKAaFM Rimar. Study of selected burner parameters on the gas-air mixture combustion. MM Sci J 2022;2022.
[33] Lei J, Liu N. Scaling flame height of fully turbulent pool fires based on the turbulent transport properties. Proc Combust Inst 2017;36(2):3139–48.
[34] Bak M, Im S, Mungal M, Cappelli M. Studies on the stability limit extension of premixed and jet diffusion flames of methane, ethane, and propane using nanosecond repetitive pulsed discharge plasmas. Combust Flame 2013;160(11):2396–403.
[35] Szegö G, Dally B, Nathan G. Scaling of NO_xemissions from a laboratory-scale mild combustion furnace. Combust Flame 2008;154(1–2):281–95.
[36] Cui Y, Li G, Xu W, Zhu J. Experimental investigation of NOx and CO emissions from fuel rich-lean flame of natural gas. Adv Mat Res 2012;347-353:3821–5.
[37] CARB. Carbon monoxide & health; Available from: https://ww2.arb.ca.gov/resources/carbon-monoxide-and-health [Accessed January 9, 2025].
[38] CARB. Nitrogen Dioxide & Health; Available from: https://ww2.arb.ca.gov/resources/nitrogen-dioxide-and-health [Accessed January 9, 2025].